Structure, epr parameters, and reactivity of organic free radicals from a density functional approach

Vincenzo Barone

Dipartimento di Chimica, Universita Federico II, via Mezzocannone 4, I-80134 Napoli, Italy

Summary. A recently introduced density functional incorporating gradient corrections and some Hartree–Fock exchange has been used to study the structures, properties, and reactivity of representative organic free radicals. A general theoretical model has been introduced, in which standardized grid, functional, and orbital basis set are used to compute geometrical parameters, vibrational frequencies, and one-electron properties. The results are compared with available experimental data from diatomic to polyatomic radicals. All the geometric and electronic parameters compare favourably with available experimental data and with the results of refined post Hartree–Fock computations. Also the thermodynamics and kinetics of a representative unimolecular reaction (isomerization of formaldehyde radical cation) are well reproduced. These findings together with the very favourable scaling of the computations with the number of electrons suggest that the density functional approach is a promising theoretical tool for the study of relationships between structure and properties of large free radicals.

Key words: Density functional theory –. Organic free radicals – Hartree–Fock exchange

Introduction

Density functional (DF) theory is by far the most useful non-empirical alternative to conventional post Hartree–Fock methods for studying structure and reactivity of molecular systems (e.g. [1–4] and references therein). The situation should be even more favourable for open-shell systems, where both the unrestricted (UHF) and the spin restricted (ROHF) Hartree–Fock wave functions often provide a poor starting point for correlation treatments. In the unrestricted Kohn–Sham (UKS) method, in contrast, the correlation functional provides a separate estimation of the correlation contribution to energy; there is thus no need to increase artificially the spin polarization of the doubly occupied orbitals, and the electron density is predicted with greater accuracy. This is also proven by the S^2 value for the Slater determinant of non-interacting electrons, which comes out to be much closer to the theoretical values for pure spin states [5–8].

Hyperfine splittings (hfs) are particularly sensitive to the quality of the wave function near nuclei (isotropic term) or in the whole space (anisotropic terms).

Especially the isotropic (contact) contribution is one of the most troublesome one-electron properties for quantum-mechanical computations [9–17]. Furthermore vibrational averaging effects are often significant for not too rigid systems [13, 17–19]. These considerations have stimulated our interest toward the development of a well-defined computational protocol ranging from the selection and testing of reliable electronic methods to the implementation of refined large-amplitude Hamiltonians to describe nuclear motions. While the dynamical treatment we have developed in a series of studies [17–20] can easily be applied to extended systems characterized by a limited number of large amplitude vibrations, the situation is more involved for the electronic computations. In fact it is now well recognized that Hartree–Fock and perturbative correlation methods are not able to provide quantitative results [11, 15–17]. In a series of recent studies, promising results have been obtained using purposely tailored basis sets with multireference configuration interaction [21, 22], or coupled cluster [14, 17, 21] methods. In the latter case, it has also been shown that there is little difference between different implementations of the exponential ansatz, or between ROHF and UHF zeroth-order wave functions [12, 23].

Only qualitative trends have been reproduced in a number of studies with the UKS formalism in the framework of the local spin density (LSD) approximation [24–26]. Much improved results have been recently obtained by at least three different groups introducing gradient corrections in the approximate exchange-correlation functional [7, 8, 27–33]. These studies show, however, a strong dependence of the results on the molecular geometry and on the choice of the auxiliary basis set used to fit Coulomb, exchange, and correlation potentials, not to speak about the convergence of the results with the dimensions of the orbital basis set. Furthermore, unusually large modifications of the results are connected to the choice of specific gradient corrections in either the exchange and correlation functionals. A first goal of this paper is thus to investigate the performance of different functionals using basis sets large enough to be considered saturated. Since those basis sets are, of course, too large to be routinely used in molecular computations, some manageable basis sets are next built, which are able to reproduce the results of the reference set.

As mentioned before, a general computational protocol for the study of open-shell systems should be able to provide, with the same method and basis set, reliable geometrical structures, thermodynamic parameters, and one-electron properties. Gradient-corrected functionals are already quite promising in this connection, and recent work shows that small modifications of the functional form [4] or partial inclusion of the Hartree–Fock exchange [34–36] can provide even better results. I have been especially interested in the second approach, since both the theoretical motivation, and the computational results are particularly convincing. Although partial retention of the Hartree–Fock exchange has been originally justified by Becke [35] on the grounds of the connection theorem [37], I offer here another piece of motivation. In fact, even gradient corrected functionals retain a local from, so that at least part of the non-local contributions are still neglected [7, 32, 33]. If we make the reasonable assumption that these terms are essentially operative for parallel spin electrons, it makes sense that they are more or less proportional to HF exchange.

The original application of hybrid functionals did not involve full self-consistency, nor geometry optimization. In fact stand-alone DF programs never compute HF exchange, which is most easily added only at the end of the iterative SCF procedure. The situation is different for codes derived from standard HF packages,

like the GAUSSIAN92/DFT [38] system of programs I am using. In fact these programs manage to remove HF exchange after full computation of the standard Fock matrix. There is, therefore, no computational advantage in neglecting the information contained in this term. Furthermore, the convergence of the SCF process is enhanced for hybrid methods retaining at least part of HF exchange. It would seem that this approach has a heavier dependence (N^4) on the number of basis orbitals than the claimed N^3 dependence of the standard DF codes [2]. It has been, however, repeatedly shown [3] that much slower $(N^{2.5})$ increases of computational times can be obtained for large molecules by properly programmed HF approaches, and pseudospectral techniques can bring the HF approach to the same asymptotic behaviour as the KS method. Furthermore, even if the computational times of the hybrid procedures should remain somewhat larger than standard ones, they are still feasible and would be worthy of consideration if able to provide significantly improved results. Here I will show that this is actually the case especially for open shell systems. To this end I report a number of representative examples selected to point out the strengths and limitations of the proposed approach. The discussion is, therefore, limited to this aspect, without introducing chemical considerations, even if they would be, in some cases, very interesting.

A much more ambitious target is the characterization of reactive potential energy surfaces (PES). There is, in fact, the suspicion that, in spite of its acknowledged merits in the description of covalent bonds, the DF approach could still suffer from difficulties in coping with subtle energy differences. Some recent studies have shown that structures and strengths of standard hydrogen bridges [39, 40] and electron deficient bonds [41] are well described and the same happens for simple bond fissions [42]. The situation is also promising for transition structures [40–45], although some problem remains for processes involving proton transfer [46]. The performances of several density functionals in this field have been investigated by a parallel DFT and post Hartree–Fock study of the isomerization of formaldehyde cation radical to hydroxymethylene radical.

2 Method

All KS computations have been performed by the Gaussian 92/DFT system of programs [38]. Particular characteristics of this code are the use of Gaussian basis functions, the avoidance of auxiliary functions, the implementation of effective pruned grids, and the availability of analytical first and second derivatives [3, 47, 48]. On the basis of some test computations with very large grids, the standard SG-1 grid [47] has been selected for the present study.

Local spin density (LSD) computations have been carried out using the uniform electron gas (ueg) exchange [49] and the Vosko, Wilk and Nusair (VWN) correlation [50] functionals. Gradient corrections have been introduced using the Becke exchange part [51], and either the Perdew [52] or the Lee-Yang-Parr [53] correlation parts. Following the standard nomenclature, the former calculations will be referred to in the following as BP, and the latter as BLYP. Note that the Perdew correlation functional is added to the VWN one, whereas the LYP functional replaces also the VWN contribution. Computations involving the combined use of Perdew-Wang exchange [54] and Perdew [52] correlation potentials will be referred to as PWP.

The original Becke 3 parameter functional [35] (referred to as B3PW) has the form:

$$E^{B3P} = A\,E_x^{ueg} + (1-A)\,E_x^{HF} + E_c^{local} + B\,\Delta E_x^{Becke} + C\Delta E_c^{Pw91}, \qquad (1)$$

where the constants $A = 0.80$, $B = 0.72$, and $C = 0.81$ are determined by fitting the heats of formation of a standard set of molecules [35]. When replacing the Perdew-Wang correlation functional by the LYP one (to obtain the B3LYP functional), it must be taken into account that the latter functional includes both local terms and gradient corrections. As a consequence, the VWN correction (E_c^{VWN}) is used to provide the excess local correlation required, and Eq. (1) becomes:

$$E^{B3LYP} = A(E_x^{Slater}) + (1 - A)E_x^{HF} + B\Delta E_x^{Becke} + CE_c^{LYP} + (1 - C)E_c^{VWN}. \quad (2)$$

A number of test computations has shown that the same parameters can be used in B3PW and B3LYP functionals, and that the latter generally provides better results.

The quality of DF results has been further tested with reference to post Hartree–Fock (second-order Moller Plesset perturbation, MP2 [55], and coupled clusters with single and double replacements, CCSD, in some cases including perturbative inclusion of triples, CCSD(T) [56]). In the case of open shell systems, evaluation of correlation energy can start from unrestricted (leading to UMP2 [55] and UCCSD(T) [57] methods) or spin restricted (leading to ROMP2 [58] and ROCCSD(T) [59, 60] methods). Both formalisms have been employed in this study, although the restricted approach I use [58–60] has the advantage that spin contamination makes no contribution to the energy to any perturbation order. All the post Hartree–Fock computations were carried out using the ACES II package [61]. In all cases all orbitals were correlated.

2.1 Basis sets

A full double-ζ polarized basis set is the smallest reasonable starting point for hfs determination since each highly occupied orbital requires a partner spin polarization orbital that is localized on roughly the same region of space, but is typically a little more diffuse [62]. In the context of conventional *ab inito* methods, Chipman showed [16] that, partly due to some error compensation, the popular Huzinaga–Dunning double-ζ basis set (hereafter referred to as DZ) [63, 64] can give reliable results if augmented by standard polarization functions [65] (DZP basis set). More stable results are obtained uncontracting the outer core-inner valence region of heavy atoms [16] and adding a very tight s function to hydrogen [66]. Increased flexibility (needed to describe, for instance, halogen atoms [17]) is obtained on going to a triple-ζ contraction of valence orbitals and adding a set of s, p diffuse functions [67] on non-hydrogen atoms. The resulting (10, 6, 1;5,1)/(5,3,1;3,1) basis set (hereafter referred to as TZP') has been fully validated in recent post Hartree–Fock studies of fluoromethyl [17] and nitroxide [19] radicals. Here we have further added to all atoms a tight s function with orbital exponent six times that of the more compact function of the original basis set.

The definition of a general computational protocol requires, in my opinion, that the same method and (if possible) basis set be used for geometry optimization, determination of (harmonic) force fields and computation of spectroscopic properties. According to some recent work [1,4], converged geometries and thermodynamic quantities are obtained only starting from triple-ζ basis sets augmented by double sets of polarization functions. At this level, different primitive sets and contraction patterns are essentially equivalent. Taking into account all the above requirement I guess that a (11,6,2;6,2)/[6,4,2;3,2] basis set (hereafter referred to as TZ2P') would perform quite well. Finally, computation of reliable multipolar moments and polarizabilities requires also the inclusion of a set of diffuse polariza-

tion functions. I have, therefore, optimized the contraction coefficients of the resulting TZ2P$^+$ basis set through UKS computations on atoms. Addition of f functions on non-hydrogen atoms (tested in some cases) is denoted by addition of a f suffix to the above labelings. Note that all the polarization and diffuse functions are taken from the recent correlation consistent basis sets developed by Dunning [67]. Some test computations have been performed also by other standard basis sets, including the split valence polarized set of Ref. [65] (referred to as SVP) and the 6-31G** [68], 6–311G** [69] and 6–311$^+$ G** [70] set developed by Pople and coworkers.

We then need some very large basis set, which can be used as reference to test the convergence of the results. For non-hydrogen atoms I have selected the (14, 9, 4, 3) basis set recently used to develop density matrix averaged ANO basis sets [71], and for hydrogen the $8s$ set of Ref. [72] supplemented by a tight s function ($\zeta = 2683.0$), a diffuse s function ($\zeta = 0.027962$) and the $4p$, $3d$ polarization set of Ref. [71]. Once again a tight s function (with orbital exponent five times the most compact one of the original basis set) has been added to all atoms. The resulting basis set (referred to as EXT) has been left completely uncontracted in all the benchmark computations.

2.2 Spin dependent properties

The formulae for calculating hyperfine parameters are obtained from the spin Hamiltonian [73],

$$H_{\text{spin}} = -g_e \beta_e S_z B_z - g_N \beta_N I_z B_z + STI.$$

The first two contributions are the electronic and nuclear Zeeman terms, respectively, and arise from the interactions between a magnetic field B and the magnetic moments of the unpaired electrons (S_z) or the magnetic nuclei (I_z) in the system. The remainder is the hyperfine interaction term, and is a result of the interactions between the unpaired electrons and the nuclei. β_e, β_N are the electron and nuclear magnetons, and g_e, g_N the electron and nuclear magnetogyric ratios.

The 3×3 hyperfine interaction tensor T can be further separated into its isotropic (spherically symmetric) and anisotropic (dipolar) components. Isotropic hyperfine splittings $A_{\text{iso}(N)}$ are related to the spin densities $\rho^s(r_N)$ at the corresponding nuclei by

$$A_{\text{iso}}^{(N)} = \frac{8\pi}{3} \frac{g_e}{g_0} g_N \beta_N \sum_{\mu,\nu} P_{\mu,\nu}^{\alpha-\beta} \langle \varphi_\mu | \delta(r_{kN}) | \varphi_\nu \rangle.$$

Computation of these terms is straightforward and is already included in most *ab initio* codes.

The anisotropic components are derived from the classical expression of interacting dipoles:

$$A_{ij}^{(N)} = \frac{g_e}{g_0} g_N \beta_N \sum_{\mu,\nu} P_{\mu,\nu}^{\alpha-\beta} \langle \varphi_\mu | r_{kN}^{-5} (r_{kN}^2 \delta_{ij} - 3r_{kN,i} r_{k,Nj}) | \varphi_\nu \rangle.$$

These terms are more complicated to compute, and also to determine experimentally. They are, however, strictly related to field-gradient integrals already available in several standard *ab initio* packages. For linear molecules, the molecular symmetry axis is chosen as one of the components say Z. Since the tensor is traceless, there remains only one meaningful diagonal element, say T_{ZZ} with

$T_{ZZ} = -2T_{XX} = -2T_{YY}$. The quantity A_{dip}, defined by $A_{dip} = \frac{1}{2} T_{ZZ}$ is called the dipolar hyperfine coupling constant. The observed hyperfine structures of epr spectra of linear molecules are often analyzed in terms of the components of the hyperfine tensor parallel $(A\|)$ and perpendicular $(A\perp)$ to the bond. These are related to the above A_{iso} and A_{dip} through $A\| = A_{iso} + 2A_{dip}$ and $A\perp = A_{iso} + (T_{XX} + T_{YY})/2$ [73]. Frosch and Foley introduced a different set of parameters a, b, c, and d to describe the hyperfine interaction in diatomic molecules [74]. These parameters, preferred by microwave spectroscopists, are related with A_{iso} and A_{dip} as $A_{iso} = b + c/3$ and $A_{dip} = c/3$. In the present paper we will treat the isotropic (hereafter referred to simply as a_N) and the anisotropic (hereafter referred to as A) hyperfine coupling constants separately.

EPR spectra are often analyzed on the basis of the effective Zeeman coordinates or the principal axes of the g tensor, so that if the principal axes of the hyperfine tensor and the g tensor do not coincide, the off-diagonal elements of the hyperfine tensor have non-zero values. In such a case diagonalization of the hyperfine tensor gives the eigenvalues of A_{XX}, A_{YY}, and A_{ZZ}. In microwave spectroscopy, the hyperfine coupling constants of polyatomic molecules are analyzed on the basis of the principal axes of the moment of inertia (a, b, c). Unfortunately, the off-diagonal elements often fail to be determined experimentally, and only the diagonal elements, A_{aa}, A_{bb}, and A_{cc} are obtained. However, when the off-diagonal values are given, the principal values of the anisotropic hyperfine tensor, A_{XX}, A_{YY}, and A_{ZZ} can be obtained by diagonalizing the matrix.

The hfc are usually given in units of MHz by mw spectroscopist, and in Gauss or mT (1 G = 0.1 mT) by epr spectroscopists. In the present work all the theoretical hfc are given in Gauss; to convert data to MHz one has to multiply by 2.8025 g_0/g_e, where g_0 is the g factor of the electron in individual radicals.

3 Results and discussion

3.1 Validation

As a first step basis set saturation effects have been investigated for a representative biatomic open shell system, namely the $^3\Sigma^-$ state of NH. The hyperfine structure of NH is experimentally well characterized [75, 76] and several theoretical studies have been also performed [22, 66, 77–79]. We compare in Table 1 our B3LYP results with experiment and with the recent complete active space (CAS) multiconfiguration self-consistent (MC-SCF) results of Ref. [22]. The results of Table 1 deserve the following comments:

(1) XH bond lengths (which are consistently overestimated by DF methods [27, 34]) are now quite reliable.

(2) Hydrogen Fermi splittings and anisotropic coupling constants are not particularly demanding, whereas the situation is much worse for the Fermi term of the N atom.

(3) Standard split valence and double ζ polarized basis sets provide very low values, which are somewhat increased by diffuse functions; a significant improvement is then afforded by decontraction of the inner valence outer core part of the basis set.

(4) Essentially converged results are obtained by the TZ2P' basis set, except for the dipole moment, which is particularly sensitive to the addition of diffused functions on the N atom.

Table 1. Selected properties of the $^3\Sigma^-$ state of NH (see text for details)

Basis set	r	μ	$\omega(I)$	A_{iso} N	A_{iso} H	A_{dip} N	A_{dip} H
B3LYP/SVP	1.050	1.634	3256(35)	9.0	−20.2	7.6	11.3
B3LYP/DZP	1.050	1.632	3257(35)	4.6	−20.2	7.6	11.3
B3LYP/DZP[a]	1.048	1.700	3270(31)	5.7	−20.3	7.6	11.3
B3LYP/DZP'	1.045	1.671	3241(33)	6.3	−20.6	7.6	11.3
B3LYP/DZP'[a]	1.044	1.530	3239(29)	7.0	−20.9	7.9	11.4
B3LYP/TZ2P'	1.045	1.675	3260(23)	6.3	−20.5	7.9	11.4
B3LYP/TZ2P'[a]	1.040	1.525	3261(21)	6.4	−20.0	8.0	11.1
B3LYP/TZ2P'f	1.040	1.593	3257(23)	6.4	−20.3	8.0	10.8
B3LYP/TZ2P'f[a]	1.040	1.525	3260(20)	6.4	−19.8	8.0	10.8
B3LYP/EXT	1.039	1.522	3255(20)	7.1	−20.0	8.2	10.9
ROHF/DZP[b]	1.036[e]	/	/	18.3	−32.2	7.3	12.4
CISD/DZP[b]	1.036[e]	/	/	13.3	−21.2	7.2	11.5
CAS/DZP[b]	1.036[e]	/	/	14.8	−23.9	7.2	11.7
SCF/EXT'[b,c]	1.036[e]	/	/	13.4	−34.9	7.6	11.8
CAS/EXT'[b,c]	1.036[e]	/	/	5.9	−23.9	7.6	11.0
EXP[d]	1.036	1.39	/	6.9	−23.6	8.1	10.9

[a] Bond length (r in Å), dipole moment (μ in D), harmonic wave number and IR intensity (ω in cm^{-1} and values in parenthesis in km mol^{-1}), isotropic (A_{iso} in G) and anisotropic (A_{dip} in G) coupling constants; [b] from Ref. [22]; [c] the EXT' basis set is comparable to our EXT one (see Ref. [22]); [d] bond length and dipole moment quoted in Ref. [3], hfs from Ref. [76]; [e] fixed at the experimental value

A detailed comparison of different density functionals for the complete characterization of open-shell systems has been next performed for the methyl radical. From an experimental point of view, the structure [80], atomization energy [4], vibrational frequencies [81], and EPR parameters [82–85] of this radical are well characterized. Also the theoretical literature is very rich [86–89]. A further advantage of this species is that, as for other hydrocarbon radicals, relatively small basis sets provide essentially converged results [17]. The data reported in Table 2 show that the isotropic ^{1}H couplings are well described at all levels of theory, as are the various anisotropic parameters. At the ^{13}C atom, however, the different functional forms generate different electron density distributions, and thus different hyperfine couplings are obtained, It has been shown [7, 33, 90, 91] that gradient corrections give a build-up of unpaired spin-density at the core- and outer-valence regions of the heavy atoms relative to LSD, and also generate a slightly lower spin density at the hydrogens. The different gradient corrected functionals behave in a quite similar way, although computations of other systems suggest that PWP [7, 8, 28, 31] and B3LYP [92, 93] functionals are generally more reliable. The effect of vibrational averaging on the hyperfine structure of CH$_3$ has been also computed by the procedure described in detail in Ref. [17]. The results reported in Table 2 confirm that the effect is particularly significant for the carbon atom and point out the reliability of DF methods also in this connection.

Several theoretical studies of H$_2$AB radicals have been reported since these systems include the essential local characteristics of σ (e.g. H$_2$BO, H$_2$CN, H$_2$CO$^+$) or π (e.g. H$_2$CF, H$_2$CO$^-$, H$_2$NO) radicals and are small enough to be studied by very refined methods. Spin densities at β protons of σ radicals are particularly hard to be correctly reproduced by standard *ab initio* methods. The results obtained by the B3LYP/TZ2P' model for H$_2$CO$^+$ are compared in Table 3 with those

Table 2. Selected properties of methyl radical obtained by different methods and basis sets (see text for details)

Parameter[a]	B3LYP EXT	B3LYP DZP'	B3LYP TZ2P'	LSD TZ2P'	BP TZ2P'	BLYP TZ2P'	UMP2[b] TZP'	UCCSD(T)[b] TZP'	EXP
CH	1.077	1.083	1.079	1.088	1.087	1.085	1.079	1.082	1.079[c]
De	1300	1287	1300	1435	1331	1350	/	/	1286[d]
S^2	0.754	0.753	0.754	0.752	0.754	0.753	0.755	0.750	0.750
A_{iso}C	31.1	30.3	29.8	10.9	23.0	27.2	25.5	27.8	
A_{iso}H	−23.1	−22.5	−23.3	−18.1	−22.8	−21.7	−25.3	−24.6	
A_{dip}C	29.0	26.5	27.5	26.9	27.4	27.8	/	/	
A_{dip}H	14.4, 0.6	14.3, 0.3	14.3, 0.1	13.8, 0.1	14.0, 0.2	14.0, 0.1	/	/	
$\langle A_{iso}C \rangle$	40.9	40.2	39.6	20.8	32.9	37.1	35.4	37.7	22.5[e], 21.8[f]
$\langle A_{iso}H \rangle$	−21.1	−20.5	−21.3	−16.1	−20.8	−19.7	−23.3	−22.6	12.5, 0.5[g] 38.3[h] −23.1[h]

[a] Bond length in Å, atomization energy (De) in kJ mol^{-1}, expectation value of spin squared, and hyperfine couplings in G. For isotropic hyperfine couplings both equilibrium (planar) and vibrationally averaged ($\langle \rangle$) values are given; [b] from Ref. [17]; [c] Ref. [80]; [d] Ref [4]; [e] Ref. [82]; [f] Ref. [83]; [g] Ref. [84]; [h] Ref. [81]

Table 3. Selected properties of H_2CO^+ radical obtained by different methods and basis sets (see text for details)

Para-meter[a]	PWP[b,c] IGLO-III	PWP[d] TZ2P'	B3LYP TZ2P'	B3LYP 6-311G**	MP2 6-311G**	CCSD 6-311G**	CISD[e,f] [8,4,1/6,1]	SAC-CI[f,g] DZ	SAC-CI[f,h] STO	2R-CIS[f,i] DZ'	EXP[j]
CO	1.189	1.207	1.189	1.188	1.195	1.201	1.210	1.210	1.210	1.210	/
CH	1.129	1.134	1.118	1.121	1.111	1.115	1.100	1.100	1.100	1.100	/
HCO	118.2	120.4	120.1	120.1	118.7	119.4	124.0	124.0	124.0	124.0	/
A_{iso}H	133.3(117.0)	125.7	132.8(128.9)	120.2	102.8	107.2	86.2	117.1	119.4	91.8	132.7
A_{iso}C	−31.8(−28.1)	−29.7	−33.5(−32.0)	−34.2	−37.8	−38.8	−24.7	−28.8	−29.8	−29.9	−38.8
A_{iso}O	−12.6(−13.4)	−14.4	−16.6(−16.9)	−10.3	−15.8	−20.3	−12.6	−13.3	−19.9	−17.3	/

[a] Bond lengths in Å, bond angle in degrees, isotropic hyperfine splittings in Gauss; [b] from Ref. [7]; [c] hfs in parenthesis are obtained at the following geometry: CO = 1.210; CH = 1.100; HCO = 124.0; [d] from Ref. [28]; [e] from Ref. [9]; [f] the geometry was not optimized; [g] from Ref. [94]; [h] from Ref. [95]; [i] from Ref. [96]; [j] from Ref. [97]

obtained by several other methods [9, 11, 94–96] and with experiment [97]. It is apparent that the hfs of hydrogen atoms are in fairly good agreement with experimental results, and are more realistic than those obtained by post Hartree–Fock methods. The other hfs are, at least, of the same quality as those obtained by CIS computations.

In conclusion the preference for the B3LYP model with respect to other gradient corrected functionals essentially stems from the more reliable structures and formation enthalpies obtained by this model. This is particularly significant for unstable open-shell species for which experimental structures are often unreliable if not simply unavailable.

3.2 Vinyl and 2-fluorovinyl radicals

As is always the case for unsaturatēd σ radicals, the theoretical reproduction of the hyperfine structure of vinyl [81, 82] and 2-fluorovinyl [98, 99] radicals (see Fig. 1) is particularly demanding. They provide, therefore, a significant benchmark for new computational models. The structures and harmonic force fields of ethylene, fluoroethylene, acetylene and fluoroacetylene obtained by the B3LYP model are comparable with MP2 values, which, in turn, are particularly accurate for these systems [100]. This is particularly significant for CH and CF bond lengths, which are poorly reproduced by standard DF methods [3–5, 27]. When going to the corresponding open shell systems, the quality of the MP2 model strongly deteriorates, whereas this is not the case for the B3LYP method. As shown in Table 4, the B3LYP harmonic frequencies approach the level of those obtained by a much more expensive model coupling MP2 and CCSD force constants [100]. It is worth noting that the force constant of CC stretching increases going from ethylene to vinylic systems, whereas those of CH stretchings decrease for β hydrogens, and increase for the α one. These behaviors are reflected, of course, in the bond lengths: for instance the CC bond length diminishes from 1.317 in fluoroethylene to 1.300 Å in fluorovinyl, while the CH distance increases from 1.080 to 1.086 Å for H_β, and decreases to 1.072 Å for H_α.

The difficulties met by standard methods for the computation of hfs in unsaturated σ radicals are well reflected by the data of Table 5. For instance, the UMP2 coupling constant of C_β has the wrong sign (11.8 vs. − 8.6 G) and the hfs of H_{anti} is about 30 G below the experimental value. The comparable performances of fourth order perturbative results (UMP4) indicate that perturbative methods are of
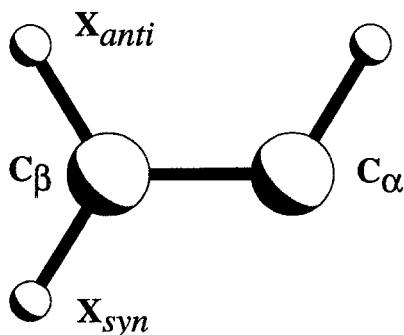

Fig. 1. Atom labeling for substituted vinyl radicals.

Table 4. Harmonic wave numbers (cm^{-1}), zero point (ΔZPE), electronic (ΔV), and ground state vibrationally adiabatic (ΔV_{ag}) energy differences (kJ mol^{-1}) for the syn and anti structures of 2-fluorovinyl

	Syn			Anti		
	UHF[a]	Best[b]	B3LYP	UHF[a]	best[b]	B3LYP
1a' (CH$^\alpha$)	3476	3367	3316	3472	3365	3314
2a' (CH$^\beta$)	3380	3233	3135	3429	3281	3186
3a' (CC)	1651	1676	1673	1627	1649	1645
4a' (H$^\beta$ CC)	1396	1310	1289	1403	1332	1312
5a' (CF)	1209	1146	1080	1179	1103	1039
6a' (H$^\alpha$ CC)	907	810	722	956	846	757
7a' (FCC)	539	513	475	490	465	421
1a'' (wag)	847	985	820	924	1042	883
2a'' (twist)	721	800	639	705	841	679
ΔZPE	0.0	0.0	0.0	0.4	0.5	0.5
ΔV	0.0	0.0	0.0	1.0	1.0	0.9
ΔV_{ag}	0.0	0.0	0.0	1.4	1.5	1.4

[a] 6-31G** basis set; [b] mixed UMP2 and UCCSD force field with a 6-311$^+$ G** basis set, see Ref. [100]

Table 5. Hyperfine coupling constants (in Gauss) obtained by different methods for vinyl and 2-fluorovinyl radicals. All the HF and post-HF computations employ the DZP basis set, whereas B3LYP computations are performed with the TZ2P' basis set

Atom	ROHF	UHF	UMP2	UMP4	CCSD	CCSD(T)	B3LYP	Exp.[a]
Vinyl								
C$^\alpha$	124.2	187.5	112.5	115.5	127.4	124.3	109.5	107.6
C$^\beta$	12.3	− 46.7	11.8	7.1	− 6.8	− 5.7	− 5.0	(−)8.6
H$^\alpha$	20.3	− 18.0	19.3	18.7	10.1	10.9	17.6	13.3
H$^\beta$c	11.8	48.0	21.0	21.9	29.9	29.8	42.5	34.2
H$^\beta$t	24.0	68.0	41.3	43.0	51.4	51.8	66.2	68.5
Anti2-fluorovinyl								
C$^\alpha$	118.0	178.9	100.6	104.3	118.8	116.2	105.1	101.4
C$^\beta$	25.4	− 33.1	44.3	34.5	15.0	16.7	18.9	18.3
F	54.9	41.0	108.1	102.2	93.0	98.0	108.5	73.0
H$^\alpha$	6.5	− 30.5	9.0	8.4	1.4	0.7	1.7	< 1
H$^\beta$	17.9	34.9	0.1	3.0	13.1	12.7	18.6	38.1
Syn 2-fluorovinyl								
C$^\alpha$	112.7	177.4	97.6	101.8	114.8	111.4	98.4	101.4
C$^\beta$	5.4	− 63.5	5.9	− 1.6	− 19.4	− 18.1	− 17.1	18.3
F	29.7	− 6.2	62.7	56.4	47.7	51.5	72.0	73.0
H$^\alpha$	5.4	− 30.9	6.9	6.6	− 2.6	− 2.1	1.0	< 1
H$^\beta$	14.5	53.8	15.4	23.7	34.1	34.1	41.2	38.1

[a] hfs of vinyl from Refs. [81, 82]; hfs of 2-fluorovinyl from Ref. [98]

marginal utility and more refined (and expensive) models are needed. This is confirmed by the reasonable results obtained by the coupled cluster approach (note that the results for vinyl are essentially converged, whereas more extended

basis sets would be necessary for fluorine [17,100]). On the other hand, PWP [27] and B3LYP results are in good agreement with experimental findings, the largest discrepancy being about 8 G. Also the isotropic hyperfine coupling constants of 2-fluorovinyl are shown in Table 5. At the B3LYP level the experimental substitutent effect is reproduced and the quantitative agreement is satisfactory.

From another point of view, in the case of 2-fluorovinyl, one intuitively expects the anti configuration to be preferred in order to minimize the direct spatial interaction of the electronegative fluorine atom with the unpaired electron. B3LYP and post Hartree–Fock computations indicate, on the contrary, that the two structures are essentially isoenergetic (see Table 4) and the computed hyperfine splittings of the syn-isomer (especially with respect to the β substituents) are in better agreement with experiment (see Table 5). Since zero point energy increases the relative stability of the syn isomer, I suggest that in this case chemical intuition provides the wrong answer.

3.3. Isomerization of the formaldehyde radical cation

I wish to conclude this analysis of the performances of the B3LYP/TZ2P' computational model by considering a reactivity problem. Several recent studies have pointed out the relevance of the isomerization between normal and distonic forms of oxygen containing radical cations [101]. Furthermore the correct reproduction of the thermodynamic and kinetic characteristics of such equilibria are very demanding from a computational point of view [102]. The prototype of these systems (i.e. the formaldehyde radical cation) is small enough to allow very refined computations, thus being an ideal benchmark for the B3LYP approach.

Table 6 collects the computed geometrical and energetic parameters for the formaldehyde radical cation (FRC), its distonic form, the hydroxymethylene radical cation (HMRC), and the first order saddle point (SP) connecting them (see also Fig. 2). In the case of FRC, the B3LYP CO bond length (1.188 Å) is shorter than the post Hartree–Fock (1.195 and 1.194 Å at the MP2 and CCSD levels, respectively) and standard DF (1.192 and 1.194 Å at the BP and BLYP levels, respectively) values. An even shorter value is obtained by the LSD approach. On the contrary the C–H distances obtained by the B3LYP model (1.121 Å) are longer than post Hartree–Fock values (1.111 and 1.115 Å at the MP2 and CCSD level, respectively). The difference is, however, much lower than with standard DF approaches, which, as already noted, provide X–H distances longer than post-HF values by as much as 0.02 Å. These results are not surprising because in the case of neutral formaldehyde the B3LYP/TZ2P' model gives a CO bond length (1.201 Å) shorter than that obtained by post-HF (CCSD 1.205 Å) and standard gradient corrected DF (BP 1.210 Å) methods, but in remarkable agreement with the experimental value (1.203 Å). The same effect is also present for CH bond lengths. These trends still hold for HMRC, but the differences are smaller. In fact the CO distance is 1.217 Å at the B3LYP level, whereas the CCSD and BLYP values are 1.224 and 1.229 Å, respectively. Upon reduction of the standard DF results by 0.02 Å, the CH and OH lengths are nearly equal at any level of computation. The same considerations hold also for the SP, whose geometrical parameters are roughly equal by MP2 and B3LYP computations.

As previously reported [101, 102], the MP2 method incorrectly predicts that the FRC/HMRC isomerization is endothermic by 8.4 kJ mol^{-1}. Also the activation energy (about 170 kJ mol^{-1}) is significantly underestimated. Both these effects

Table 6. Optimized bond length (Å), valence angles (degrees), and relative stabilities (kJ mol^{-1}) for the formaldehyde radical cation, its distonic form and the corresponding saddle point (SP)

	H$_2$CO$^+$							SP							HCOH$^+$						
Method	MP2	QCISD	LSD	BP	BLYP	B3LYP	B3LYP	MP2	QCISD	LSD	BP	BLYP	B3LYP	B3LYP	MP2	QCISD	LSD	BP	BLYP	B3LYP	B3LYP
basis	TZP	TZP	TZP	TZP	TZP	TZP	TZ2P	TZP	TZP	TZP	TZP	TZP	TZP	TZ2P	TZP	TZP	TZP	TZP	TZP	TZP	TZ2P
CO	1.195	1.201	1.175	1.192	1.194	1.188	1.188	1.210	1.219	1.213	1.226	1.228	1.213	1.211	1.222	1.224	1.213	1.227	1.229	1.217	1.216
CH	1.111	1.115	1.147	1.135	1.133	1.121	1.118	1.104	1.106	1.125	1.119	1.117	1.109	1.107	1.098	1.101	1.118	1.112	1.111	1.102	1.101
OH								1.233	1.233	1.235	1.238	1.242	1.233	1.234	0.989	0.985	1.006	1.002	1.003	0.992	0.990
HCO	118.7	119.4	121.9	121.0	121.0	120.1	120.1	137.1	134.8	134.6	134.6	134.3	134.7	134.8	124.5	124.5	124.1	123.8	123.8	124.6	124.7
HOC								58.0	58.4	57.8	57.8	57.8	58.1	58.1	116.4	116.8	120.2	118.5	119.6	119.1	118.9
ΔE	0.0	0.0	0.0	0.0	0.0	0.0	0.0	171.5	205.0	177.0	188.8	196.3	202.1	201.7	-8.4	27.6	28.4	33.1	35.5	28.9	27.6

H_2CO^+ SP $HCOH^+$
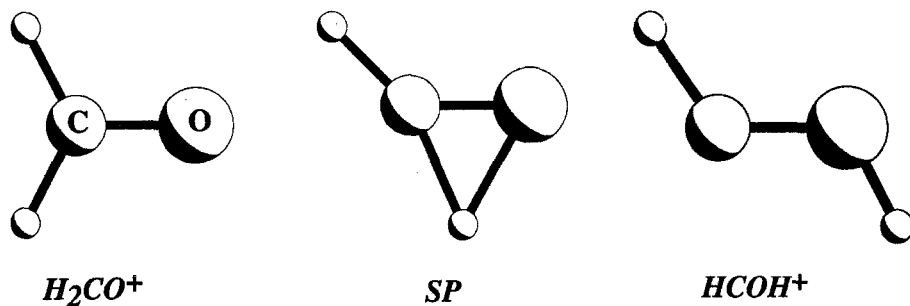
Fig. 2. Schematic drawing of stationary points on the potential energy surface governing isomerization of formaldehyde radical cation

are related to a poor description of the FRC electronic structure [92]. LSD and B3LYP endothermicities are close to the CCSD value of $27.6 \, kJ \, mol^{-1}$, whereas BLYP and BP models overestimate the reaction energy by as much as $8 \, kJ \, mol^{-1}$. All the DF activation energies are close to the CCSD result ($205.0 \, kJ \, mol^{-1}$), but this time the LSD approach underestimates the value ($177.0 \, KJ \, mol^{-1}$) with respect to gradient corrected functionals (196, 198 and $202 \, kJ \, mol^{-1}$ from BLYP, BP, and B3LYP computations, respectively). Although zero point energies do not alter the general trend at any level of computation, it is gratifying that the values obtained from CCSD and B3LYP computations are nearly identical, whereas lower values are generally obtained at the MP2 level.

All the above results seem to indicate that the B3LYP functional is more reliable than standard DF approaches concerning both geometrical and energetic parameters, giving values which are comparable to the much more expensive CCSD results.

4. Conclusion

The present paper explores the reliability of a new density functional on a number of structural, spectroscopic, and reactivity problems involving organic free radicals. Introduction of some Hartree–Fock exchange in gradient corrected functionals provides structures, harmonic force fields, and thermochemical data approaching chemical accuracy. The situation is even better concerning spin dependent properties where B3LYP computations with properly tailored basis sets often outperform the accuracy of the most sophisticated many body models. In essence, self-consistent hybrid methods like B3LYP seem to couple the advantages of local (good geometries) and gradient corrected (good one-electron properties and energetic quantities) functionals with an improved overall accuracy.

Although further work is needed concerning the transferability of these trends to large classes of systems, the first results suggest that the B3LYP/TZ2P' computational model is a promising theoretical tool for the study of large organic radicals.

References

1. Ziegler T (1991) Chem Rev 91:651
2. Andzelm J, Wimmer E (1992) J Chem Phys 96:1280

3. Johnson BG, Gill PMW, Pople JA (1993) J Chem Phys 98:5612
4. Laming GJ, Termath V, Handy NC (1993) J Chem Phys 99:8765
5. Laming GJ, Handy NC, Amos R (1993) Mol Phys 80:1121
6. Baker J, Scheiner A, Andzelm J (1994) Chem Phys Lett 216:380
7. Eriksson LA, Malkina OL, Malkin VG, Salahub D (1994) J Chem Phys 100:5066
8. Adamo C, Barone V, Fortunelli A, J Phys Chem (in press)
9. Feller D, Davidson ER (1984) J Chem Phys 80:1006 (1984)
10. Feller D, Davidson ER (1991) In: Maksic ZB (ed) Theoretical models of chemical bonding, Part 3, Springer, Berlin
11. Sekino H, Bartlett RJ (1985) J Chem Phys 84:4225 (1985).
12. Perera SA, Watts JD, Bartlett RJ (1994) J Chem Phys 100:1425
13. Carmichael I (1987) Chem Phys 116:351
14. Carmichael I (1989) J Chem Phys 91:1072
15. Carmichael I (1991) J Phys Chem 95:6198
16. Chipman DM (1992) Theoret Chim Acta 82:93 and Refs. therein
17. Barone V, Minichino C, Grand A, Subra R (1993) J Chem Phys 99:6787
18. Barone V, Minichino C, Faucher H, Subra R, Grand A (1993) Chem Phys Lett 205:324
19. Barone V. Grand A, Minichino C, Subra R (1993) J Phys Chem 97:6355
20. Barone V, Jensen P, Minichino C, (1992) J Mol Spectrosc 154:439
21. Feller D, Glendening ED, McCullough Jr EA, Miller RJ (1993) J Chem Phys 99:2829
22. Fernández B, Jørgensen P, McCullogh Jr EA, Symons J (1993) J Chem Phys 99:5995
23. Barone V (submitted)
24. Akai H, Akai M, Blügel S, Drittler B, Ebert H, Terakura K, Zeller R, Doderichs PH (1990) Progr Theor Phys (Suppl) 101:11
25. Mattar SM, Hamilton WD (1992) J Phys Chem 96:1606
26. Mattar SM, Brewer SE (1992) J Phys Chem 96:1611
27. Barone V, Adamo C, Russo N (1993) Chem Phys Lett 212:5
28. Barone V, Adamo C, Russo N (1994) Int J Quantum Chem 52:963
29. Ishii N, Shimizu T (1993) Phys Rev A 48:1691
30. Eriksson LA, Malkin VG, Malkina OL, Salahub DR (1993) J Chem Phys 99:9756
31. Kong J, Eriksson LA, Boyd RJ (1993) Chem Phys Lett 217:24
32. Austen MA, Eriksson LA, Boyd RJ (1994) Can J Chem 72:695
33. Wang J, Eriksson LA, Boyd RJ, Shi Z, Johnson B (1994) J Phys Chem 98:1844
34. Beckc AD (1993) J Chem Phys 98:1372
35. Becke AD (1993) J Chem Phys 98:5648
36. Barone V, Adamo C (1994) Chem Phys Lett 224:432; 228:499 (E)
37. Harris J, Jones RO (1974) J Phys F4:1170; Gunnarson O, Lundquist BT (1976) Phys Rev B13:4274; Harris J, (1984) Phys Rev A29:1648; Becke AD, (1988) J Chem Phys 88:1053
38. Frisch MJ, Trucks GW, Head-Gordon M, Gill PMW, Wong MW, Foresman JB, Johnson BG, Schlegel HB, Robb MA, Replogle ES, Gomperts R, Andres JL, Raghavachari K, Binkley JS, Gonzalez C, Martin RL, Fox DJ, DeFrees DJ, Baker J, Stewart JJP, Pople JA (1993) GAUS-SIAN92/DFT, Gaussian Inc., Pittsburgh, PA
39. Mijoule C, Latajka Z, Borgis D (1993) Chem Phys Lett 208:364
40. Barone V, Orpanolini L, Adamo C (1994) Chem Phys Lett 230:189
41. Barone V, Adamo C, Russo N, Fliszar S (1994) Chem Phys Lett 222:597
42. Lee AM, Handy NC (1993) J Chem Soc Far Trans 89:3999
43. Sosa C, Lee C (1993) J Chem Phys 98:8004
44. Deng L, Ziegler T, Fan L (1993) J Chem Phys 99:3823
45. Stanton RV, Mertz Jr KM (1994) J Chem Phys 100:434
46. Johnson BG, Gonzales CA, Gill PMW, Pople JA, (1994) Chem Phys Lett 221:100
47. Gill PMW, Johnson BG, and Pople JA (1993) Chem Phys Lett 209:506
48. Johnson BG, Frisch MJ (1993) Chem Phys Lett 216:133
49. Dirac PAM (1930) Proc Cambridge Phil Soc 26:376
50. Vosko SH, Wilk L, and Nusair M (1980) Can J Phys 58:1200
51. Becke AD (1988) Phys Rev B38:3098
52. Perdew JP (1986) Phys Rev B33:8822

53. Lee C, Yang W, Parr RG (1988) Phys Rev B37:785
54. Perdew JP, Wang Y (1986) Phys Rev B33:8800
55. Pople JA, Seeger R, Krishnan R (1977) Int J Quantum Chem Symp 11:149
56. Bartlett RJ, Watts JD, Kucharsky SA, Noga J (1990) Chem Phys Lett 165:513
57. Pople JA, Head-Gordon M, Raghavachari K, (1987) J Chem Phys 87:5968
58. Knowles PJ, Andrews JS, Amos RD, Handy NC, Pople JA (1991) Chem Phys Lett 186:130
59. Rittby M, Bartlett J (1988) J Phys Chem 92:3033
60. Watts JD, Gauss J, Bartlett RJ (1992) Chem Phys Lett 200:1
61. Stanton JF, Gauss J, Watts JD, Lauderdale WJ, Bartlett RJ (1992) Int J Quantum Chem 26:879
62. Chipman DM (1989) Phys Rev A 39:475
63. Huzinaga S, (1965) J Chem Phys 42:293
64. Dunning TH Jr, (1970) J Chem Phys 53:2823
65. Dunning TH Jr, Hay PJ (1976) Modern theoretical chemistry, Ch. 1. Plenum, New York, pp 1–28
66. Chipman D, (1989) J Chem Phys 91:5455
67. Dunning TH Jr, (1989) J Chem Phys 90:1007
68. Hehre WJ, Ditchfield R, Pople JA (1972) J Chem Phys 56:2257
69. Krishnan R, Binkley JS, Seeger R, Pople JA (1980) J Chem Phys 72:650
70. Clark T, Chandrasekhar J, Spitznagel GW, Schleyer PVR (1983) J Comput Chem 4:294
71. Widmark PO, Malmquist PA, Ros BO (1990) Theor Chim Acta 77:291
72. van Duijneveldt FB (1970) IBM technical research report RJ945
73. Weltner W Jr (1983) Magnetic atoms and molecules. van Nostrand, New York and references therein
74. Frosch RA, Foley HM (1952) Phys Rev. 88:1337
75. van den Heuvel FC, Meerts WL, Dymanus A (1982) Chem Phys Lett 92:215
76. Ubachs W, ter Meulen JJ, Dymanus A (1984) Can J Phys 62:1374
77. Bender CF, Davidson ER (1969) Phys Rev 183:23
78. Kristiansen P, Veseth L (1986) J Chem Phys 84:6336
79. Engels B, Peyerimhoff SD (1989) Mol Phys 67:583
80. Hirota E, Yamada C (1985) J Mol Spectrosc 96:175 and references therein
81. Fessenden RW, Schuler RH (1963) J Chem Phys 39:2147
82. Fessenden RW (1967) J Phys Chem 71:74
83. Rogers MT, Kispert LD (1967) J Chem Phys 46:221
84. Janecka J, Vyas HM, Fujimoto M (1971) J Chem Phys 54:3229
85. Shiga T, Yamaoka M, Lund A, Naturforsch Z (1974) Teil A 29:653
86. Ellinger Y, Pauzat F, Barone V, Douady J, Subra R (1980) J Chem Phys 72:6390
87. Botschwina P, Flesch J, Meyer W (1983) Chem Phys 74:321
88. Cramer CJ (1991) J Org Chem 16:5229
89. Pacansky J, Koch W, Miller MD (1991) J Am Chem Soc 113:317
90. Tschinke V, Ziegler T (1988) Can J chem 67:480
91. Fan L, Ziegler T (1991) J Chem Phys 94:6575
92. Barone V (1994) Chem Phys Lett 226:392
93. Barone V (1994) J Chem Phys 101:6834
94. Momose T, Nakatsuji H, Shida T (1988) J Chem Phys 89:4185
95. Nakatsuji H, Izawa M (1989) J Chem Phys 91:6205
96. Nakano T, Morihashi K, Kikuchi O (1992) Bull Chem Soc Jpn 65:603
97. Knight LB, Steadman J (1984) J Chem Phys 80:1018
98. Shiotani M, Nagata Y, Sohama J (1982) J Phys Chem 86:4131
99. Raghunathan P, Sur SK (1983) J Phys Chem 87:3383
100. Barone V, Minichino C (in preparation)
101. Coitino EL, Lledos A, Serra R, Bertran J, Ventura ON (1993) J Am Chem Soc 115:9121 and references therein
102. Ling N, Smith BJ, Radom L (1992) Chem Phys Lett. 193:386